NASA Technical Memorandum 86194

Solar Maximum

Solar Array Degradation

Tom Miller

AUGUST 1985

NASA

[redacted]

NASA Technical Memorandum 86194

Solar Maximum

Solar Array Degradation

Tom Miller
Goddard Space Flight Center
Greenbelt, Maryland

National Aeronautics
and Space Administration

**Scientific and Technical
Information Branch**

1985

NASA STI
RECEIVED

CONTENTS

Page

INTRODUCTION 1

ARRAY DESCRIPTION 1

ARRAY POWER CALCULATIONS 2

METHODOLOGY 10

RESULTS 11

CONCLUSIONS 15

REFERENCES 16

INTRODUCTION

The Solar Maximum Mission (SMM) was launched February 14, 1980 aboard a Delta rocket from the Eastern Test Range, Florida. The spacecraft was injected into a 574 km circular orbit at a 33° inclination. Solar Maximum has an orbital period of approximately 96 minutes with an eclipse varying between 28 and 35 minutes. The spacecraft was designed for a lifetime requirement of two years and a lifetime duration goal of four years. Its mission is to monitor gamma ray, x-ray, ultraviolet radiation from the sun, and solar constant values. The sun pointing Solar Maximum was the first satellite to use the Multimission Modular Spacecraft (MMS) design.

Array Description

The Solar Array System (SAS) for SMM was designed, built, and tested by Hughes Aircraft Company according to NASA-Goddard specification S-409-1.[1] The solar array output power requirements were 1540 watts after two years in orbit at the winter solstice and maximum temperature. Other major requirements of the SAS consisted of a deployable, non-tracking array that could be jettisoned from the spacecraft during STS shuttle retrieval operations.

To satisfy the various system constraints, the SAS consisted of two identical paddles measuring 3.50 meters × 2.21 meters. Each paddle was comprised of 3 panels; one central panel 221 cm × 104 cm × 3.8 cm and two side panels 216 cm × 104 cm × 1.9 cm. See Figure 1.[2] Since solar array deployment dynamics required a low fundamental vibrational frequency (< 2 Hz) upon deployment, an extremely rigid substrate was mandatory. The nonflexible array was fabricated using a foam filled aluminum honeycomb core and covered with graphite GY-70 face sheets. Three layers of 2.5×10^{-3} cm thick Tedlar was bonded to the graphite face sheets to insulate the solar cells from the conductive graphite.

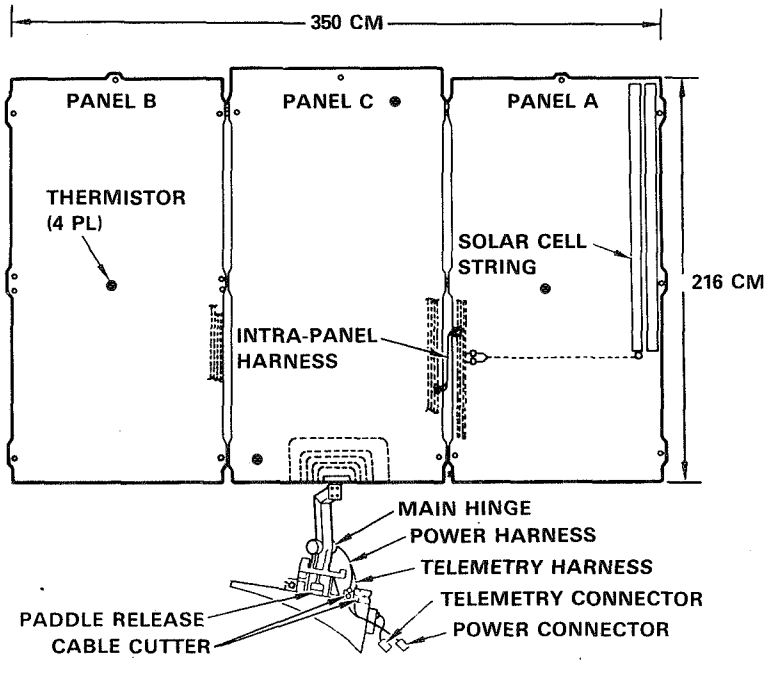

Figure 1. Paddle Description.

The electrical schematic of the array may be seen in Figure 2. Each side panel has thirteen separate strings of 134 solar cells in series and the center panel has thirteen strings of 138 cells in series. For reliability purposes, each paddle had four independent power buses. Three buses have nine parallel cell groups and one with twelve parallel cell groups. The center panel was configured differently due to the unique thermal profiles of the thicker substrate.

The 10.556 silicon solar cells on the array were manufactured by Sectrolab. The cells measured 2.0 cm × 6.2 cm with a nominal thickness of .028 cm and a .025 cm thick fused silica textured coverglass.

Table 1 features the solar cell physical characteristics.

Table 1
SAS For Solar Max Array Physical Characteristics

Solar cell	2.0 × 6.2 cm, 2.79×10^{-2} cm thick
Coverglass	7940 fused silica, 2.54×10^{-2} cm thick
Coverglass adhesive	FEP, Type C-20 Teflon®
Configuration	
Outer panel 1 ($A_1 + B_1$)	13 Np × 134 N_s
Outer panel 2 ($A_2 + B_2$)	13 Np × 134 N_s
Center panel ($C_1 + C_2$)	13 Np × 138 N_s

A key feature of these solar cells was the absence of an ultraviolet filter. This reduced the fabrication and material cost of the array. A 5.08×10^{-3} cm film of Teflon® FEP was thermally bonded to the fused silica coverglass and the silicon substrate.

The drawback of Teflon® FEP use was that exposure to ultraviolet radiation reduces its optical transmission characteristics, hence reduced electrical power output from the solar cell. Studies by TRW and NASA-Lewis Research Center have shown that an 11% loss in short circuit current resulted from exposure to ultraviolet radiation in the 0.25 μm to 0.38 μm band after 5000 equivalent sun hours with no coverglass. The specimens after irradiation were brownish in color; however, no embrittlement was evident.[3]

One problem encountered during the fabrication of the solar cells was the delamination of the Teflon® FEP from the fused silica coverglass. Although no detrimental effects on cell electrical characteristics were noticed due to the hazy film bond, 25% of the delaminated cells were replaced to assure sufficient reliability. A few cells with major delaminations remained on the array.

Array Power Calculations

In order to properly evaluate the array, the effects of illumination intensity, radiation damage, temperature, and coverglass adhesive transmission loss must be evaluated. The orbit parameters of altitude, eccentricity, and inclination affect the spacecraft's radiation environment; hence, the degradation rate of the solar cells due to charged particles. Since the spacecraft was in a nearly circular orbit, 572 km perigee to 576 km apogee, a

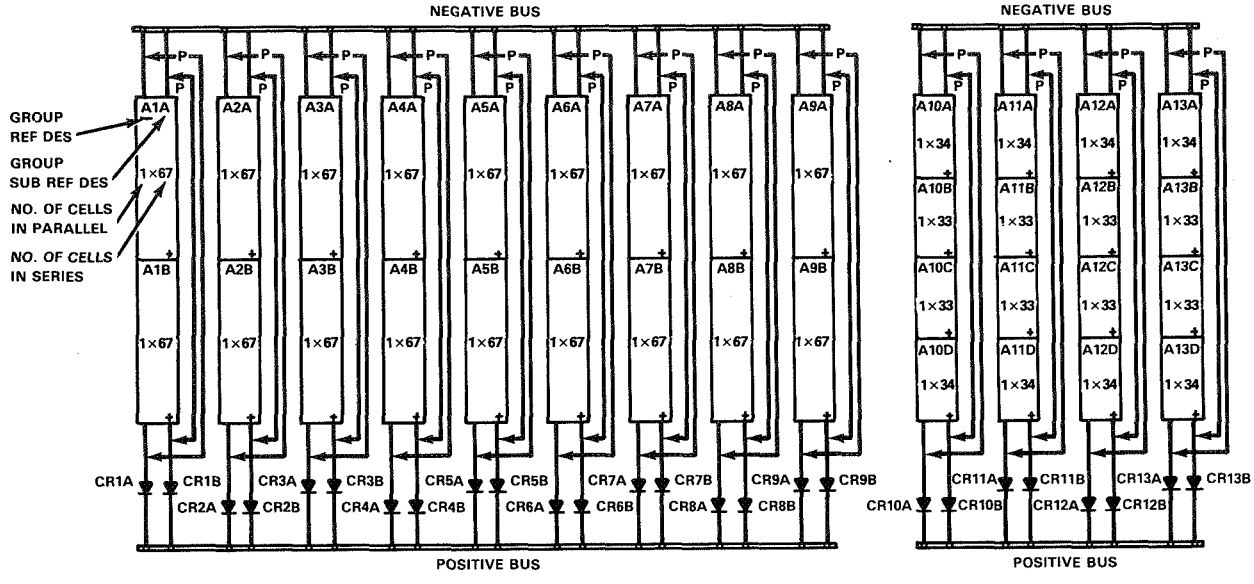

A. SIDE PANEL

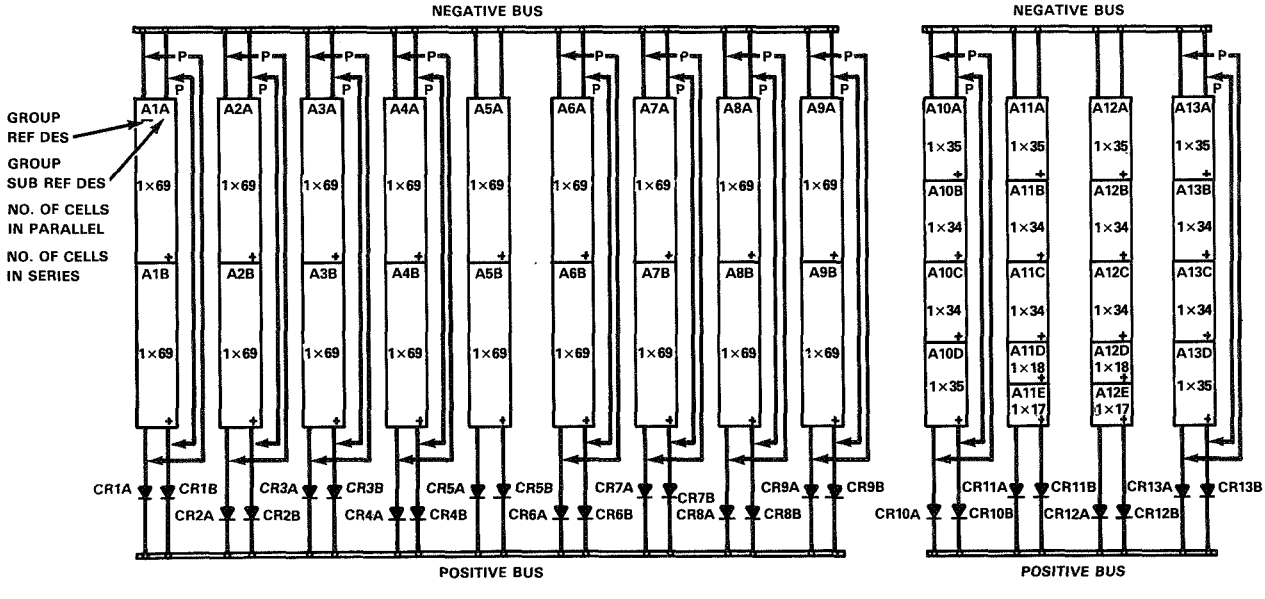

B. CENTER PANEL

Figure 2. Electrical Diagram

piece-wise orbital fit over various altitudes was not necessary. A computer program "UNIFLUX" developed by E.G. Stassinopoulos[4] calculated the omnidirectional, integral, vehicle encountered trapped particle fluxes based on space radiation models from 0.0 to 100.0 MeV. Tables 2 and 3 list the averaged flux for the different energy levels. A second computer program "SCID" by Eakin and Day[5] used the output of "UNIFLUX" to calculate the irradiation dosage for an equivalent 1 MeV electron fluence impinging on various fused silica shielding thicknesses. Figure 3 relates radiation dosage for various thickness.

Table 2
Solar Maximum Orbital Electron Flux Study Based on
AE6 Model of Composite Particle Environment

ELECTRONS			
	Composite Orbit Spectrum		
Energy Levels >(MeV)	Averaged Integ. Flux #/cm^2-sec	Averaged Integ. Flux #/cm^2-Day	Averaged Differ. Flux #/cm^2-Sec KeV
.1000	1.908E 05	1.648E 10	2.919E 03
.1250	1.508E 05	1.303E 10	1.559E 03
.2500	4.776E 04	4.126E 09	4.478E 02
.3750	1.381E 04	1.193E 09	1.204E 02
.5000	4.002E 03	3.458E 08	3.559E 01
.6250	2.022E 03	1.747E 08	1.222E 01
.7500	1.060E 03	9.155E 07	4.356E 00
1.000	4.651E 02	4.018E 07	1.383E 00
1.250	2.850E 02	2.463E 07	5.801E-01
1.500	1.752E 02	1.513E 07	3.284E-01
1.750	1.165E 02	1.006E 07	2.183E-01
2.000	7.762E 01	6.706E 06	1.276E-01
2.500	3.554E 01	3.071E 06	7.583E-02
3.000	5.987E 00	5.173E 05	4.107E-02
3.125	3.381E 00	2.921E 05	1.872E-02
3.250	1.926E 00	1.664E 05	7.884E-03
3.375	1.104E 00	9.542E 04	4.215E-03
3.500	6.352E-01	5.488E 04	0.0
3.625	3.695E-01	3.192E 04	0.0
3.750	2.158E-01	1.864E 04	0.0
3.875	1.260E-01	1.089E 04	0.0
4.000	3.235E-02	2.795E 03	0.0
4.125	1.153E-02	9.964E 02	0.0
4.250	0.0	0.0	0.0
4.375	0.0	0.0	0.0
4.500	0.0	0.0	0.0
4.625	0.0	0.0	0.0
4.750	0.0	0.0	0.0
4.875	0.0	0.0	0.0
5.000	0.0	0.0	0.0

From reference 4

Table 3
Solar Maximum Orbital Proton Flux Study Based on
AE6 Model of Composite Particle Environment

PROTONS			
	Composite Orbit Spectrum		
Energy Levels >(MeV)	Averaged Integ. Flux #/cm^2-sec	Averaged Integ. Flux #/cm^2-Day	Averaged Differ. Flux #/cm^2-Sec KeV
.1000	1.009E 03	8.715E 07	3.248E-01
.5000	8.439E 02	7.291E 07	3.016E-01
1.000	7.029E 02	6.073E 07	2.210E-01
2.000	5.438E 02	4.699E 07	1.398E-01
3.000	4.241E 02	3.664E 07	9.792E-02
4.000	3.327E 02	2.875E 07	6.978E-02
5.000	2.802E 02	2.421E 07	4.881E-02
6.000	2.394E 02	2.068E 07	3.725E-02
7.000	2.058E 02	1.778E 07	2.831E-02
8.000	1.780E 02	1.538E 07	1.969E-02
9.000	1.656E 02	1.430E 07	1.316E-02
10.00	1.542E 02	1.332E 07	1.094E-02
11.00	1.438E 02	1.243E 07	9.905E-03
12.00	1.343E 02	1.161E 07	9.097E-03
13.00	1.256E 02	1.085E 07	8.354E-03
14.00	1.176E 02	1.016E 07	7.695E-03
15.00	1.102E 02	9.521E 06	6.386E-03
16.00	1.034E 02	8.931E 06	4.057E-03
18.00	1.003E 02	8.669E 06	2.189E-03
20.00	9.744E 01	8.419E 06	1.535E-03
25.00	9.071E 01	7.838E 06	1.263E-03
30.00	8.465E 01	7.314E 06	1.122E-03
35.00	7.917E 01	6.840E 06	1.054E-03
40.00	7.418E 01	6.409E 06	9.579E-04
45.00	6.962E 01	6.015E 06	8.481E-04
50.00	6.544E 01	5.654E 06	8.072E-04
55.00	6.191E 01	5.349E 06	9.206E-04
60.00	5.860E 01	5.063E 06	7.937E-04
80.00	4.720E 01	4.078E 06	4.509E-04
100.00	3.820E 01	3.300E 06	3.321E-04

From reference 4

An annual 1 MeV equivalent electron fluence of 2.34×10^{13}/cm^2 for the outer panels and a 2.29×10^{13}/cm^2 fluence level for the center panels were ascertained. See Table 4. Thus, the maximum power output of the solar cell decreased with prolonged exposure to the space environment. See Figures 4, 5, and 6. Standardized manufacturer's specification data relate 1 MeV electron radiation effects to beginning of life solar cell maximum power current, maximum power voltage, and maximum power. Table 5 contains the actual beginning of life individual solar cell parameters averaged for both paddles. These data have been used to determine the degradation in solar cell current-voltage parameters due to charged particle irradiation. (See Table 6). The coefficients have been normalized to reflect no degradation for non-irradiated solar cells.

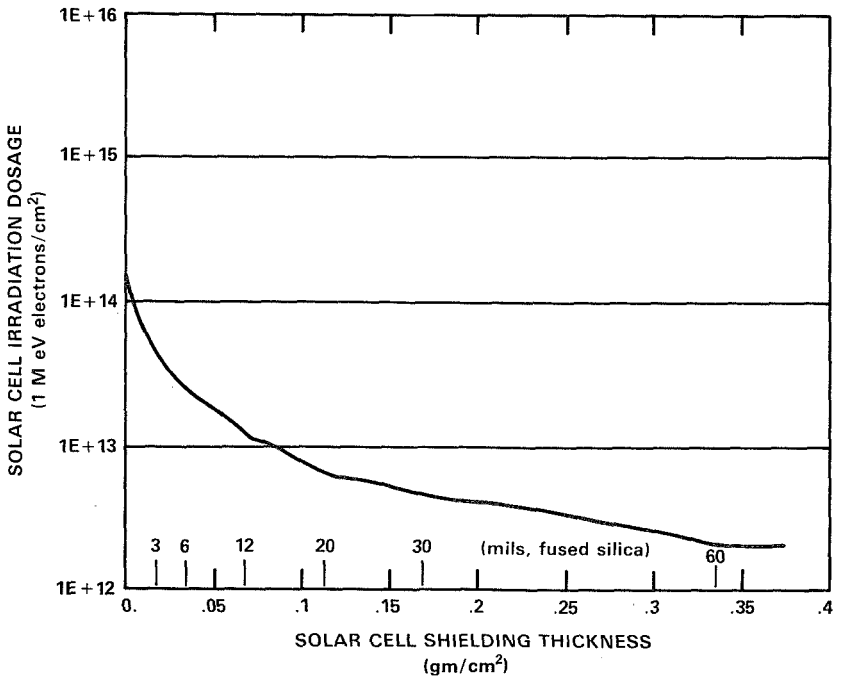

Figure 3. "SCID" Irradiation Dosage for Solar Maximum

Table 4
Predicted Annual 1 MeV Electron Fluence Environments

	Outer Panels	Center Panels
JPL Tables	$5.89 \times 10^{12}/cm^2$	$5.76 \times 10^{12}/cm^2$
NASA - GSFC	$1.29 \times 10^{13}/cm^2$	$1.23 \times 10^{13}/cm^2$
HUGHES	$2.34 \times 10^{13}/cm^2$	$2.29 \times 10^{13}/cm^2$

Table 5
SAS for Solar Max Single Cell Parameters at 28°C

Panel	Isc, Amperes	Voc, Volts	Imp, Amperes	Vmp, Volts
Outer panel 1 (A_1 + B_1)	0.4941	0.5796	0.4648	0.4812
Outer panel 2 (A_2 + B_2)	0.4914	0.5750	0.4620	0.4768
Center panel (C_1 + C_2)	0.4935	0.5802	0.4649	0.4819

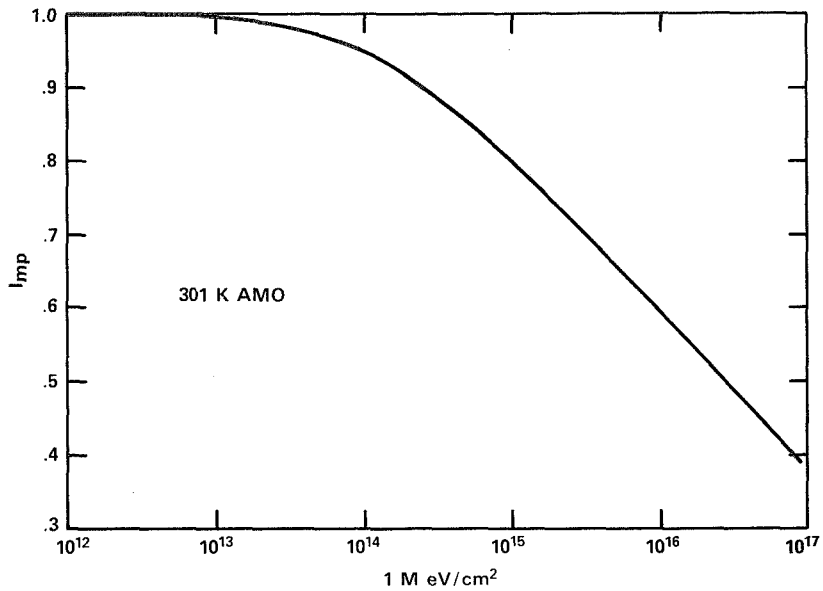

Figure 4. Maximum Power Current Coefficient vs Cumulative Radiation Dosage

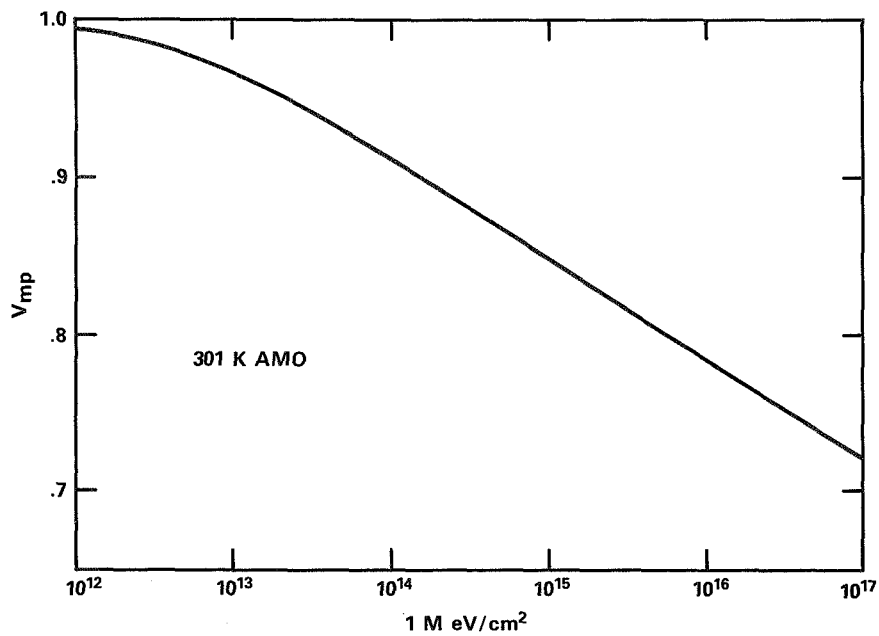

Figure 5. Maximum Power Voltage Coefficient vs Cumulative Radiation Dosage

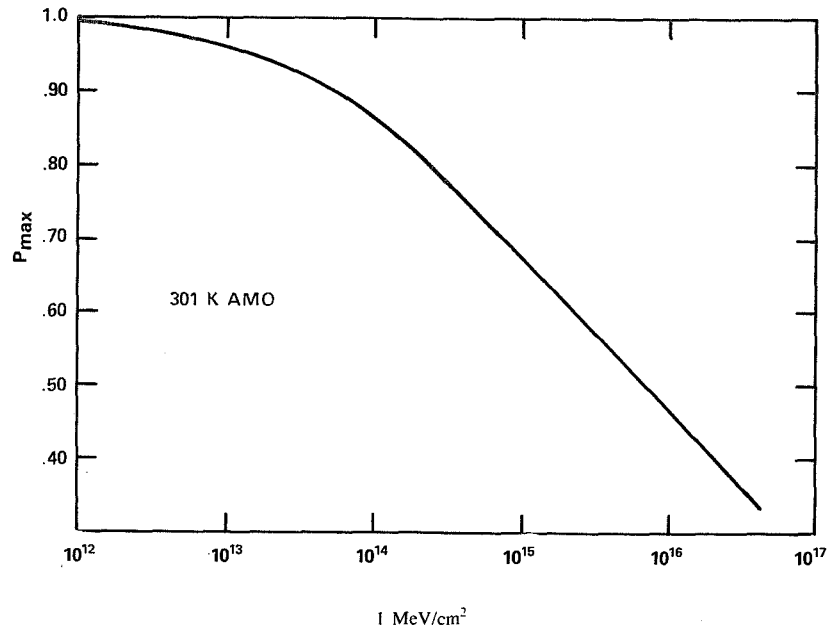

Figure 6. Maximum Power Coefficient vs Cumulative Radiation Dosage

Table 6
Solar Cell Radiation Damage Coefficients

		Years In Orbit							
	Solar Cell Parameter	0	1	2	3	4	5	6	7
OUTER PANEL	I_{SC}	1.00	.975	.960	.947	.930	.919	.910	.902
	V_{OC}	1.00	.979	.962	.952	.944	.936	.932	.928
	I_{MP}	1.00	.985	.972	.961	.950	.940	.933	.925
	V_{MP}	1.00	.946	.929	.918	.912	.906	.901	.897
	P_{MAX}	1.00	.932	.903	.882	.866	.852	.841	.830
	Fluence	0	2.34E13	4.68E13	7.02E13	9.36E13	1.17E14	1.40E14	1.64E14
CENTER PANEL	I_{SC}	1.00	.978	.961	.948	.931	.920	.912	.903
	V_{OC}	1.00	.980	.962	.953	.946	.937	.933	.928
	I_{MP}	1.00	.986	.973	.962	.952	.942	.934	.926
	V_{MP}	1.00	.948	.930	.920	.913	.907	.902	.898
	P_{MAX}	1.00	.934	.905	.885	.869	.854	.843	.832
	Fluence	0	2.29E13	4.58E13	6.87E13	9.16E13	1.15E14	1.37E14	1.60E14

Illumination intensity directly affects solar cell current. The solar constant varies with the position of the earth relative to the sun. Based on air mass zero (AMO) the solar constant has a value of 1353 W/m^2. At aphelion a 3.4% loss of intensity results. During perihelion a 3.4% increase in the solar constant value is observed. Thus seasonal fluctuations of the solar constant must be accounted for to accurately compare SMM power levels.

Temperature greatly influences solar cell performance. A reference temperature of 301.15 K (28°C) was used to characterize solar cells. At AMO maximum power current decreases at lower temperatures, while maximum power voltage increases with low temperature operation. Figures 7 and 8 depict maximum power voltage and current for various temperature and fluence profiles. Typical temperature excursions through a single orbit of SMM vary between 205 K during eclipse to 340 K when fully illuminated. Notice that the slope of the curve yields the temperature coefficient for a particular fluence level.

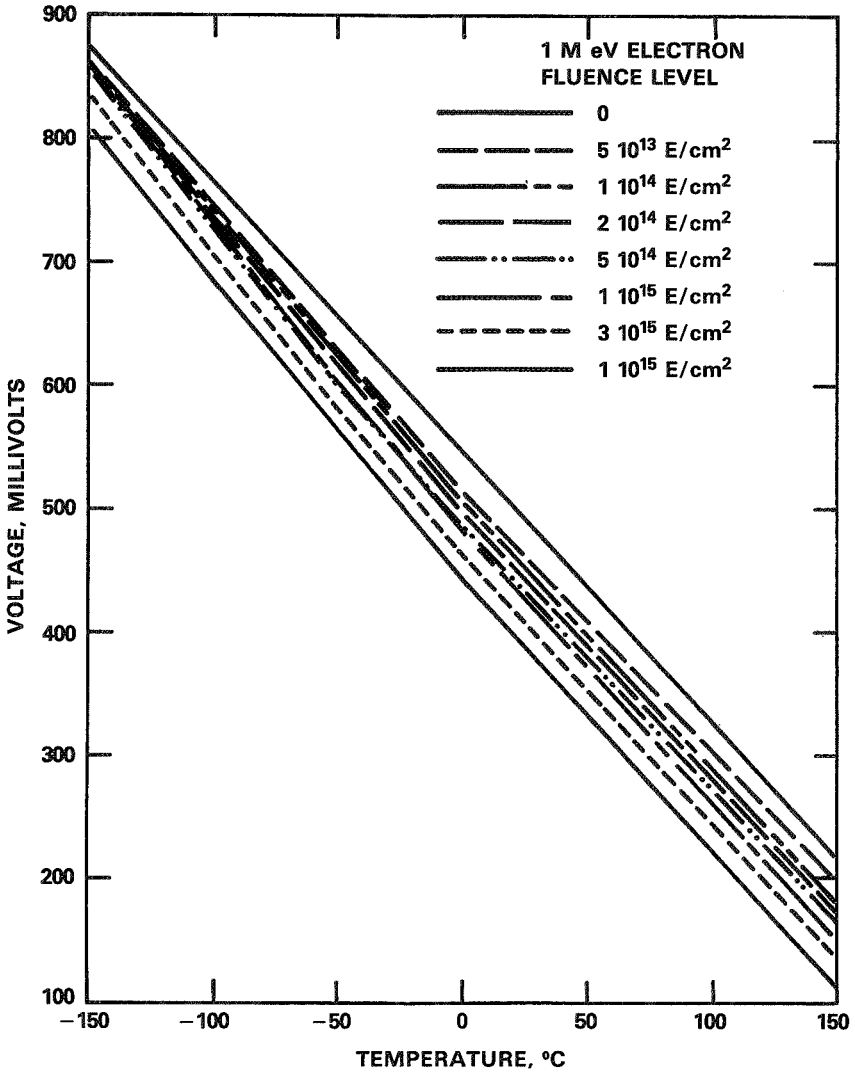

Figure 7. Maximum Power Voltage-Temperature Profile

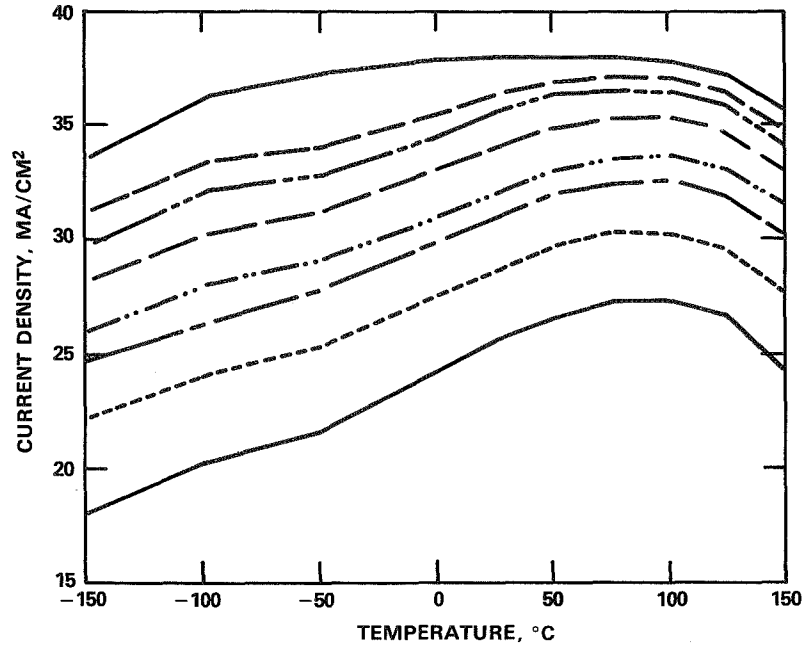

Figure 8. Maximum Power Current-Temperature Profile

METHODOLOGY

In order to evaluate the array power level throughout the mission, a prediction on maximum power was made. The prediction of maximum power for seven years in orbit was based upon Table 5 solar cell parameters. Since averaged annual radiation dosage were used in "UNIFLUX", cumulative dosage was proportional with the number of days in orbit. Equivalent fluence levels and damage coefficients for the various panels have been listed in Table 3. Maximum power was determined for the array's electrical configuration at AMO and 301.15 K.

The peak power tracking mode of the standard power regulator unit (SPRU) was used to calculate the actual array power. Immediately after eclipse, the SPRU locates the maximum power operating point of the solar array. This mode was invoked when electrical load demand at the SPRU output terminals exceeds the maximum power available from the solar array. The electrical loads consist of three twenty-two cell 20 Ampere-hour nickel-cadmium batteries and spacecraft loads. The output voltage of the SPRU and batteries were maintained at the same level. SPRU current was limited by the instantaneous power from the array. In the peak power tracking mode (PPT), the SPRU regulates the current from the array to within $\pm 5\%$ of the available maximum. When one battery reaches the selected voltage/temperature value, the SPRU changes into a voltage limit mode whereby the batteries continue to charge, but only at a taper current. Solar array current drawn decreases, thereby reducing input spacecraft power. Typically the PPT operation lasts approximately 5 minutes after dawn. During that interval, the temperature of the solar array should be in the vicinity of 250 K. Thus for comparison of observed telemetry and predicted power levels, a temperature correction factor was employed. This factor depended upon temperature and radiation fluence level.

The SMM telemetry was corrected for temperature, illumination, and radiation effects. Maximum power voltage may be obtained by the following relationship.[6]

$$V_{mp}(T_o,\varnothing,1) = V_{mp}(T, \varnothing, S) - b(\varnothing, S)(T-T_o) \quad (1)$$

where

T_o = reference temperature 301.15K

$\varnothing$ = equivalent electron radiation fluence 1 MeV/cm^2-yr

S = illumination intensity factor solar constant at AMO = 1.0

$b(\varnothing,S)$ = temperature coefficient at the given fluence level

Similarly, maximum power current was determined by the following relation:[6]

$$I_{mp}(T_o, \varnothing, 1) = \frac{I_{mp}(T, \varnothing, S)}{S} - \frac{b(\varnothing, S)}{S}(T-T_o) \quad (2)$$

On each orbit of interest, the greatest power during PPT was selected for the study. The voltage, current, and solar array temperatures were used to correct the telemetry to standard conditions. First, the current was corrected for the solar intensity. Next, the current and voltage were corrected for temperature effects. The net voltage accross 134 cells and blocking diode and total current through 13 strings per panel were multiplied together to yield maximum power output. Obtaining such information during the life of the spacecraft, array degradation can be traced with time.

A major anomaly occurred after eight months of operation. One-eighth ampere fuses in the signal conditioning assembly of the attitude control system (ACS) were improperly derated. When these fuses blew, the drive electronics to the control momentum wheels were lost. SMM orbit stability was maintained by using electromagnetic torquer bars. This method has produced a highly eliptical orbit and resulted in a $\pm$ 10° pointing precision of the spacecraft towards the sun. During this irregularity, maximum power output of the array could not be accurately assessed due to the coning of the spacecraft and possible shadowing of the solar array.

Since Solar Maximum was deisgned to be shuttle retrievable, a Solar Maximum Repair Mission (SMRM) was a major objective of STS-41C. On April 10, 1984 STS astronauts repaired the spacecraft by fixing a baffle cover on the XRP instrument, correcting the main electronics box on the coronagraph and polarimeter, and completely replacing the ACS module. This was the first time an orbiting satellite had ever been refurbished.

After release of SMM from the Shuttle, the ACS maintained the proper orbit orientation. Hence, maximum power output of the array could be validated. After reviewing initial telemetry data Hughes Aircraft Company noticed a stepwise decrease in power output from the array. This loss could have been attributed to many sources. Included were physical damage to solar cell interconnections during SMM capture and handling, or reverse biased solar cells when partial shadowing of cell strings occurred. The loss was on the order of 11% from predicted power levels. Further in-flight data was necessary to confirm this phenomena. One orbit per month was monitored for peak power output.

RESULTS

Figures 9, 10 and 11 predict Solar Maximum peak power levels at 301 K and air mass zero. The predictions also include loss factors to account for additional solar array effects. A loss in power due to ground testing was estimated at a 0.99 beginning of life value. A thermal cycling factor of 0.99 was used to account for the increased resistance of cold working intercell connections. Since no ultraviolet filter was used on the coverglass,

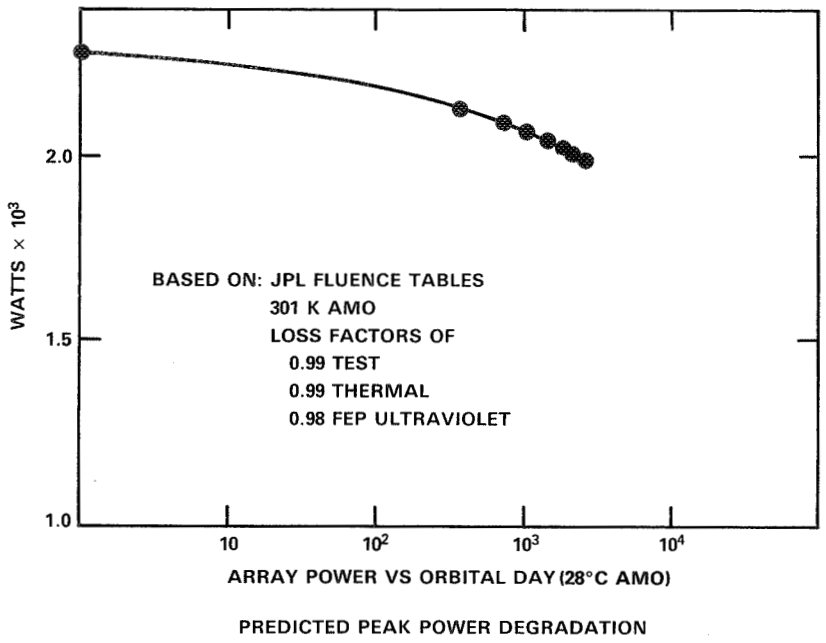

Figure 9.

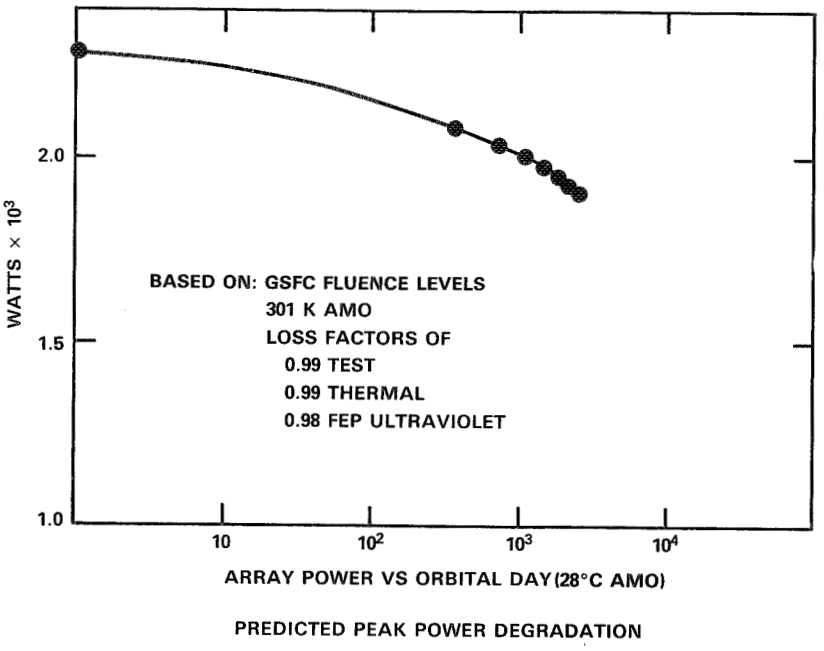

Figure 10.

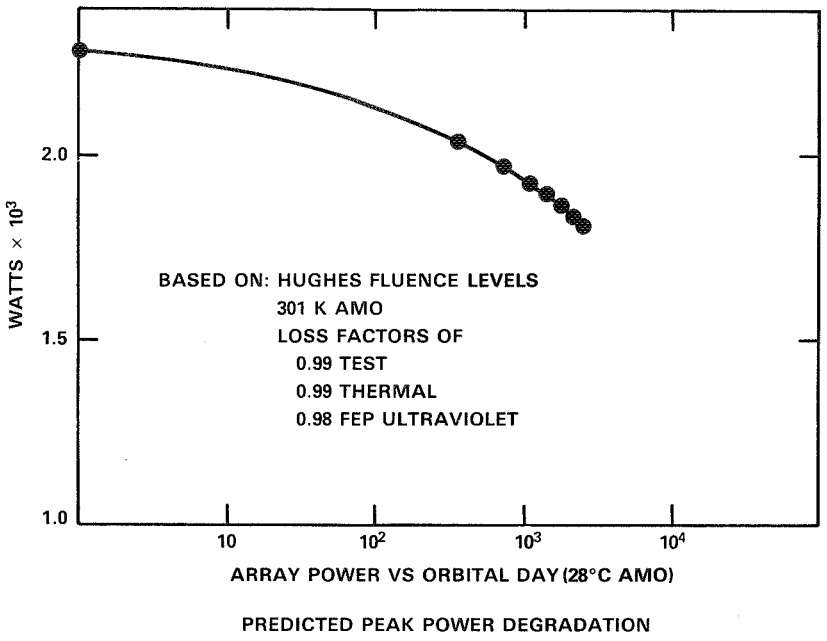

Figure 11

some darkening of the Teflon® FEP would occur. Studies at Hughes Aircraft Company indicated a contradiction on previously reported effects on Teflon® FEP. Solar cells were fabricated into test coupons according to Solar Maximum specifications and subjected to 1000 hours of ultraviolet irradiation in a low earth orbit regime. Periodic tests on the module were conducted to determine the degradation rate of the Teflon® adhesive. It was noted that after two months of exposure the loss factor had leveled off to 0.98 of the original power level. Further exposure to the ultraviolet source did not alter this value. Thus the use of the FEP as an adhesive and not as a coverglass material as reported in the literature, has a relatively high optical transmission after ultraviolet exposure. When comparing the predicted power levels, the only difference between them was the space environment fluence levels. Since the Jet Propulsion Laboratory tables were triple interpolated a possible error may have been introduced yielding a lower than actual radiation environment. This low fluence level implies a low degradation rate in solar cell power. While the models from the National Space Science Data Center at NASA - GSFC and Hughes Aircraft Company predict greater fluence levels, the models were only within a factor of two of one another. Thus the accuracy of the predictions substantially deviates upon continued exposure to the space environment.

Solar Maximum peak power tracking telemetry was plotted in Figure 12. The data was temperature compensated to 301 K. Additionally, solar constant effects were used to normalize the telemetry. Limited data was available due to archive storage problems. However, sufficient data exists to determine array power degradation. Early solar array power information was obtained from references 7 and 8. Figure 13 compares the various predictions to the actual telemetry. The general shape of the predicted curves were similar, however the Hughes model on array power matched the data most. A constant offset of approximately fifty - five watts from predicted to actual power was apparent. Although no explanation for this fact could be made, the Hughes model seems to track the telemetry data favorably.

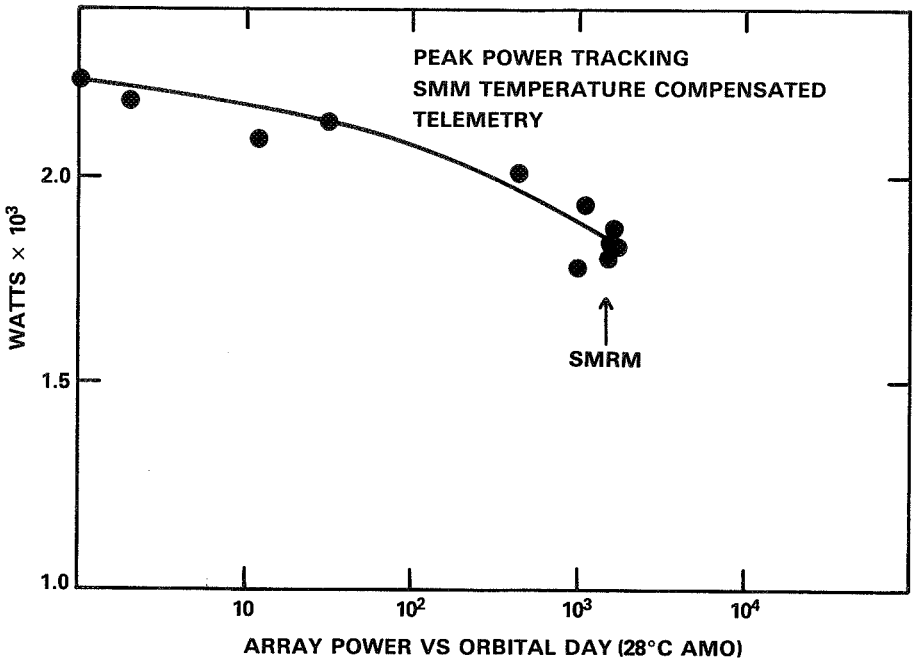

Figure 12.

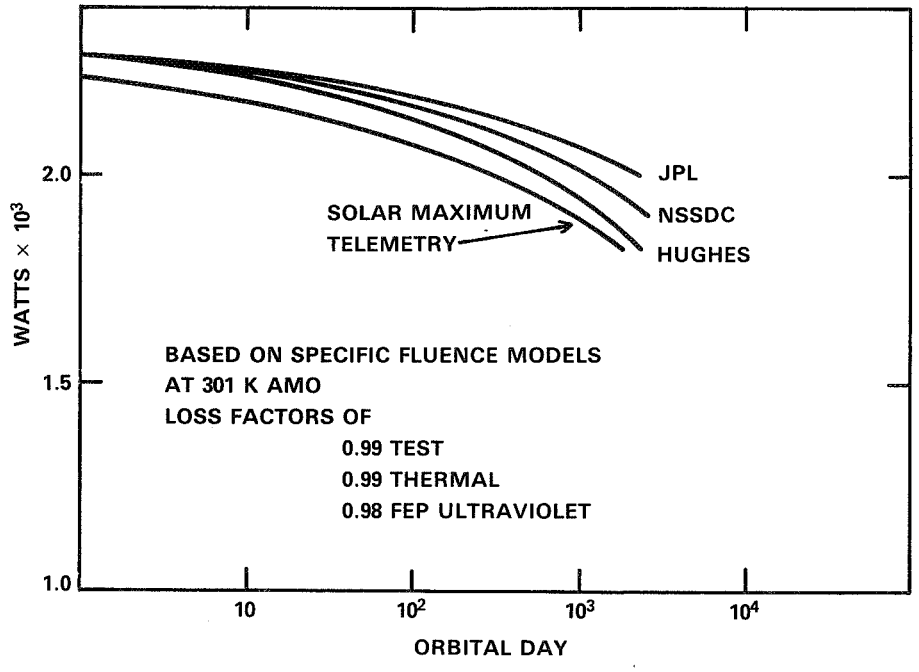

Figure 13.

Further investigation for this discrepancy has yielded the information in Figure 14. A noticeable difference in paddle current output can be observed. Reference 9 discusses a possible reason for this as a deposited residue on the #2 paddle from outgassing materials within the spacecraft body.

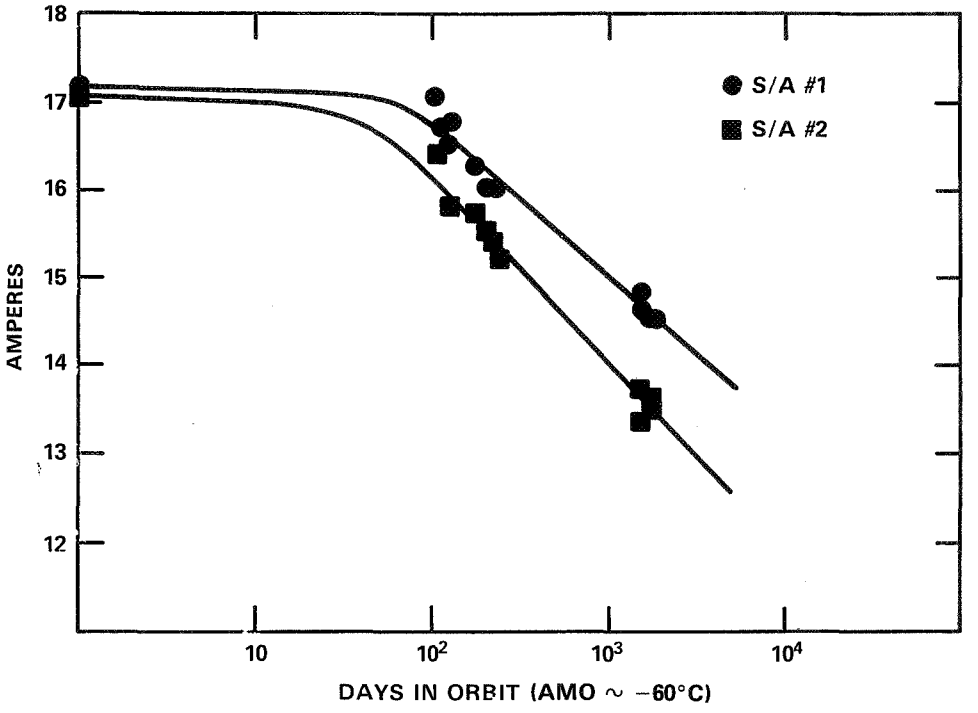

CURRENT VS TIME

Figure 14.

It should be noted that after the Solar Maximum Repair Mission, no substantial array power degradation could be detected from telemetry due to handling or shadowing of the spacecraft. A possible explanation for the initial power loss noted by Hughes Aircraft Company was that the power level obtained from telemetry was not at the maximum PPT point due to the granularity of data scanning capabilities and this gave a lowered power data point for comparison. Another explanation was that after the Solar Maximum Repair Mission, space debris consisting of bolts and other fasteners from the repaired spacecraft were floating nearby. Sunlight reflected from this debris was mistaken by the sun sensors as the true sun and permitted an improper orientation of the spacecraft. This reduction in sunlight intensity normal to the array could have been responsible for the observed loss of power noticed by Hughes.

CONCLUSIONS

The use of Teflon® FEP as a coverglass adhesive was demonstrated successfully on SMM. Although bonding problems were encountered, no effect on array performance could be ascertained. The solar array has been operating satisfactorily at slightly lower than predicted power levels. In-orbit capture and subsequent repair of SMM has extended the useful life of the spacecraft.

The initial operating capability of the Solar Maximum Solar Array was 2230 watts at 301 K and 1 solar constant at AMO. Currently the solar array has an output power of 1830 watts at reference conditions. Based upon an annual fluence rate of 2.34×10^{13} 1 MeV electron/cm^2 the Hughes model predicts an output of 1870 watts. This translates to a 2% error between telemetry and prediction.

REFERENCES

1. NASA-GSFC specification S-409-1, Solar Maximum Solar Array System, Nov. 1976. Revision A, January 1977.

2. Meese, Robert A. SMM/SAS Final Contract Report, Hughes Aircraft Company, Contract #NAS5-24208, April 1980.

3. Rauschenbach, H.S., et. al., "FEP Teflon® Encapsulated Solar Cell Modules-Further Progress," 11th IEEE Photovoltaic Specialists Conference, 1975, page 162.

4. Stassinopoulos, E.G., "Trapped Particle Environment of SMM," NASA-Goddard Space Flight Center, X-601-76-97, April 1976.

5. Eakin, V. and Day, J., "A Computer Program to Calculate Solar Cell Irradiation Dosage," NASA-GSFC X-711-84-17, September, 1984.

6. Solar Cell Radiation Handbook. Jet Propulsion Laboratory, Publication 82-69, Nov. 1982.

7. Meese, R.A., Goldhammer, L.J., and McCarthy, D.K., "Solar Array System for Solar Maximum Mission." 16th IEEE Photovoltaic Specialist Conference, 1982, page 96.

8. Wajsgrass, Harry, Grumman Aerospace, private communication.

9. Broderick, Richard J., NASA-GSFC, "In-Flight Performance of the Solar Maximum Electrical Power System," presented at the 1981 IECEC Conference, page 2129.

1. Report No.	2. Government Accession No.	3. Recipient's Catalog No.
NASA TM-86194		

4. Title and Subtitle	5. Report Date
Solar Maximum - Solar Array Degradation	August 1985
	6. Performing Organization Code: 710
7. Author(s): Tom Miller	8. Performing Organization Report No.: 85B0257
9. Performing Organization Name and Address: NASA Goddard Space Flight Center, Greenbelt, Maryland 20771	10. Work Unit No.
	11. Contract or Grant No.
	13. Type of Report and Period Covered: Technical Memorandum
12. Sponsoring Agency Name and Address: National Aeronautics and Space Administration, Washington, DC 20546	14. Sponsoring Agency Code

15. Supplementary Notes

16. Abstract

The 5-year in-orbit power degradation of the silicon solar array aboard the Solar Maximum Satellite was evaluated. This was the first spacecraft to use Teflon^{R} FEP as a coverglass adhesive, thus avoiding the necessity of an ultraviolet filter.

The peak power tracking mode of the power regulator unit was employed to ensure consistent maximum power comparisons. Telemetry was normalized to account for the effects of illumination intensity, charged particle irradiation dosage, and solar array temperature. Reference conditions of 1.0 solar constant at air mass zero (AM0) and 301 K (28°C) were used as a basis for normalization. Beginning-of-life array power was 2230 watts. Currently, the array output is 1830 watts. This corresponds to a 16 percent loss in array performance over 5 years. Comparison of Solar Maximum Telemetry and predicted power levels indicate that array output is 2 percent less than predictions based on an annual 1.0 MeV equivalent election fluence of $2.34 \times 10^{13}/cm^2$ space environment.

17. Key Words (Selected by Author(s))	18. Distribution Statement
Solar Maximum Satellite silicon solar cells Teflon^{R} FEP charged particle irradiation dosage	Unclassified - Unlimited Subject Category 20

19. Security Classif. (of this report)	20. Security Classif. (of this page)	21. No. of Pages	22. Price
Unclassified	Unclassified	18	A02

For sale by the National Technical Information Service, Springfield, Virginia 22161

GSFC 25-44 (10/77)

NASA-Langley, 1985